ELSEVIER

Journal of Alloys and Compounds 300–301 (2000) 254–260

Journal of ALLOYS AND COMPOUNDS

www.elsevier.com/locate/jallcom

Preliminary report on growth, structure and optical properties of $K_5LaLi_2F_{10}$:Ln^{3+} (Ln^{3+}–Pr^{3+}, Nd^{3+}, Er^{3+}) crystals

G. Dominiak-Dzik*, I. Sokólska, S. Gołąb, M. Bałuka

W. Trzebiatowski Institute of Low Temperature and Structure Research, Polish Academy of Sciences, 2 Okólna Street, P.O. Box 1410, 50-950 Wrocław, Poland

Abstract

Single crystals of $K_5LaLi_2F_{10}$ type containing Pr^{3+}, Nd^{3+} and Er^{3+} ions were obtained by the Bridgman method. The crystallographic structure of this stoichiometric compound (orthorhombic, space group *Pnma*) was confirmed by an X-ray diffraction analysis. Preliminary measurements of optical properties of Pr^{3+}, Nd^{3+} and Er^{3+} ions such as absorption spectra, luminescence spectra and lifetimes of main luminescent levels were done. The positions of pertinent energy levels were determined from the low temperature absorption and luminescence spectra.

Keywords: Stoichiometric compounds; Rare earth ions; Laser material; Fiber optics; $K_5LaLi_2F_{10}$ crystals

1. Introduction

$K_5LaLi_2F_{10}$ crystals belong to so-called 'stoichiometric compounds' [1] and are promising materials for obtaining high concentrations of trivalent rare earth ions substituting the La^{3+} site. The interest in stoichiometric compounds has been stimulated over last 20 years by the expectations and requirements for miniaturised laser for fiber optics. Among the stoichiometric compounds, the oxide laser materials containing Nd^{3+} such as $MeNdP_4O_{12}$ (Me=Li, Na, K), NdP_5O_{14}, $NdAl_3(BO_3)_4$, $NdNa_5(WO_4)_4$ and $K_5Nd(MoO_4)_4$ have been probably the most investigated [1–7]. However, fluoride crystals possess some advantages over oxides and there is also a great interest in the study of rare-earth containing fluorides [6–10]. Fluorides are usually transparent from the UV to the IR spectral region and have relatively low phonon energies of the order 350–500 cm^{-1}. Such low lattice frequencies prevent the effective nonradiative multiphonon relaxation to take place for most of the lanthanide excited states, improving the light emission. Particularly, the luminescent fluoride systems of $K_5LnLi_2F_{10}$ type (Ln=lanthanide ion) crystals are uncommon in that the LnF_8 polyhedra do not share fluorine atoms in the crystal structure. Consequently, rare earth (RE) ions are well isolated and spaced, so the activator–activator interaction is expected to be weak. However, results obtained for example for some Nd^{3+} or Tb^{3+} stoichiometric compounds demonstrated that self-quenching is determined to a much greater extend by crystal field strength and energy matching conditions than by RE ions separation [6,7].

Studied have been carried out on materials of the $K_5La_{1-x}Ln_xLi_2F_{10}$-type containing Nd^{3+} [11,12] and Pr^{3+} ions [13], however, polycrystalline samples only were obtained and used for these studies. In the present paper, we report on the growth of single $K_5La_{1-x}Ln_xLi_2F_{10}$ crystals (Ln — rare earth ion) containing Pr^{3+}, Nd^{3+} or Er^{3+} ions. The results of crystallographic and Raman investigations of the crystals, as well as basic optical spectroscopy, are presented.

2. Experimental

The $K_5La_{1-x}Ln_xLi_2F_{10}$ crystals (Ln=Pr^{3+}, Nd^{3+}, Er^{3+}; x=1 or 0.02 for Pr^{3+}; 1 for Nd^{3+} and 0.05 for Er^{3+}) were grown in a two stage process. In the first stage, the stoichiometric mixture of appropriate fluorides (LiF, KF, LaF_3 and LnF_3 of four 9s purity) was heated for 2 h at a temperature of 830°C in order to undergo the solid-phase reaction. At the second stage the crystals were grown by the Bridgman method in an argon atmosphere in graphite crucibles by following conditions: melting point 540°C, the temperature gradient 120 grad cm^{-1}, pulling rate 1

*Corresponding author.

0925-8388/00/$ – see front matter
PII: S0925-8388(99)00779-3

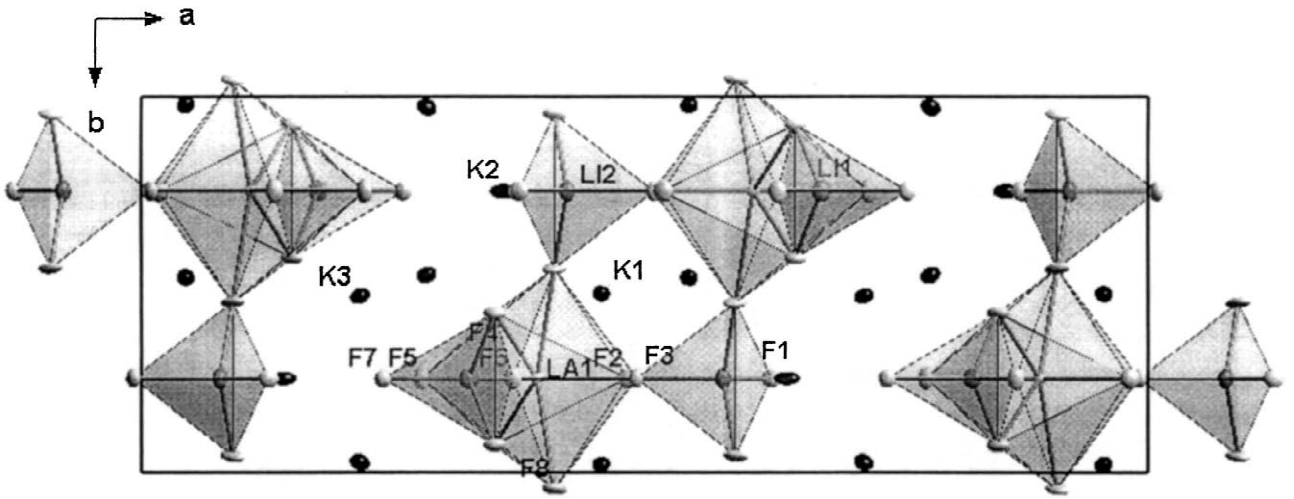

Fig. 1. Crystal structure of $K_5LaLi_2F_{10}$ in the *ab* projection.

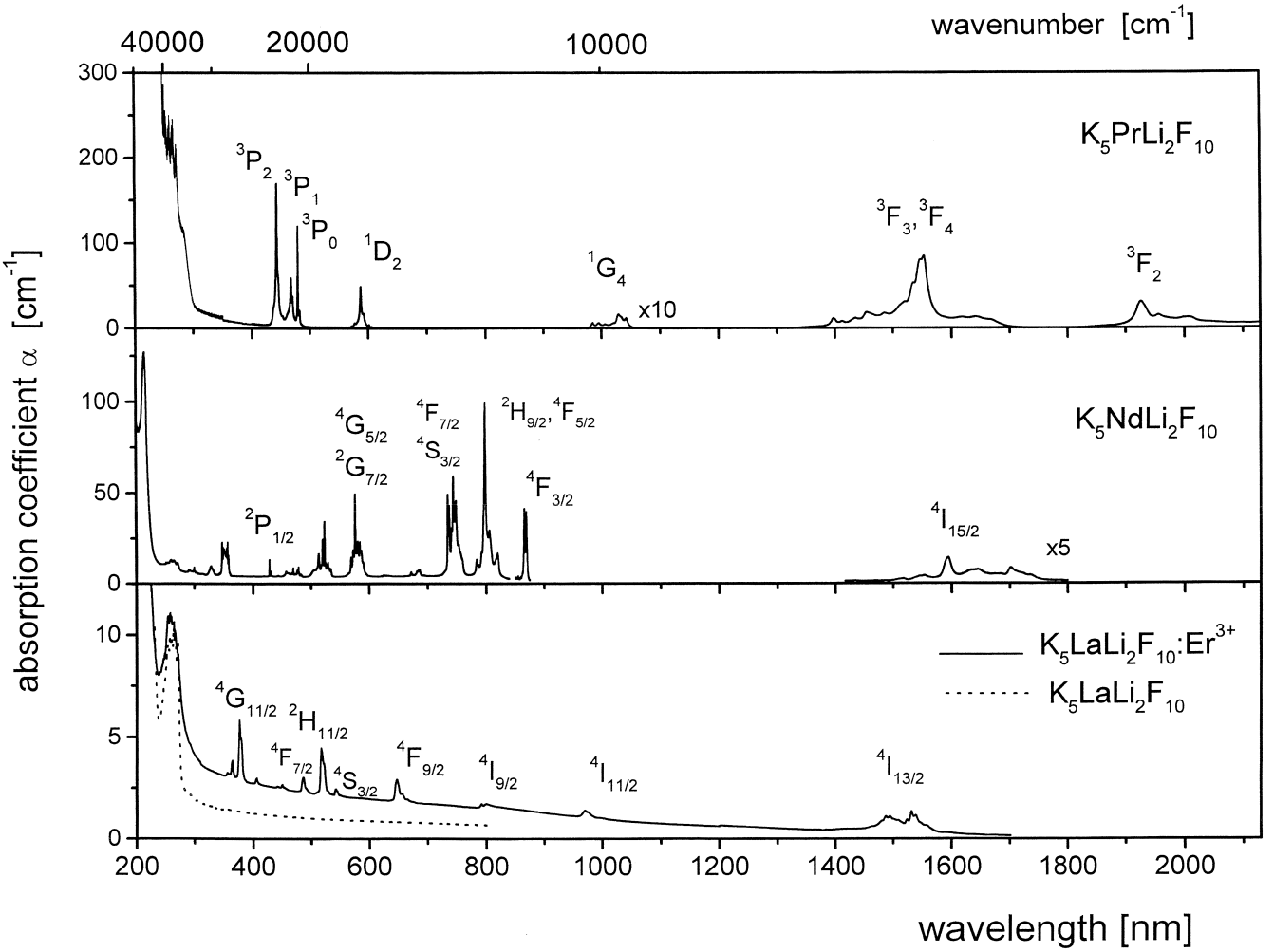

Fig. 2. Absorption spectra of $K_5LnLi_2F_{10}$ crystals with Ln = Pr^{3+}, Nd^{3+}, Er^{3+} and of $K_5LaLi_2F_{10}$ crystal (dashed line, bottom layer), $T = 300$ K.

mm h^{-1}. The crystals obtained were about 20–30 mm long and 4 mm in diameter. The crystallographic structure was determined by X-ray analysis using full automatic diffractometer with CCD detector. The energy of lattice vibrational modes was determined by Raman spectroscopy. The details of crystallographic and Raman investigation are described elsewhere [14]. Absorption spectra were measured with a Varian model 2300 spectrophotometer at 5 and 300 K with the spectral resolution of 0.2 nm in UV-VIS range and 0.8 nm in IR range. The luminescence was excited by an optical parametric oscillator (OPO) (7 ns pulse) or by an argon laser (514 nm line). The spectra were analysed in a setup consisting of a Zeiss model GDM 1000 grating monochromator, a cooled photomultiplier, a SRS 250 boxcar integrator and a personal computer. For low temperature measurements, the sample was placed in an Oxford model CF 1204 continuous flow helium cryostat equipped with a temperature controller.

3. Results and discussion

The X-ray structure determination performed on small $K_5La_{1-x}Ln_xLi_2F_{10}$ single crystals has proved the existence of one phase only. The crystal structure is orthorhombic with the space group D_{2h}^{16}–*Pnma*, full symbol $P\frac{2_1}{n}\frac{2_1}{m}\frac{2_1}{a}$. The unit cell parameters are $a=20.775$ Å, $b=7.822$ Å, and $c=6.963$ Å. The point symmetry for the La^{3+} sites was determined to be C_s. Rare earth ions enter into the $K_5LaLi_2F_{10}$ lattice replacing lanthanum ions in their sites. Lithium atoms occupy the C_s symmetry sites, whereas the symmetry of the potassium and fluorine sites is either C_s or C_1. The crystal structure (projection on *ab* plane) is presented in Fig. 1. The basic structural features of $K_5LaLi_2F_{10}$ crystal are sheets perpendicular to the *a*-axis, formed by isolated LaF_8 dodecahedra and LiF_4 tetrahedra.

In order to get information about the active lattice modes, an infrared Raman analysis was performed (for details see Ref. [14]). In spite of the expectations for the fluoride lattice modes to be low, the highest energy of vibrations (associated with the Li–F stretching vibrations) is about 685 cm^{-1}, being comparable with values for some oxide crystals.

Room temperature survey absorption spectra of the crystals investigated are presented in Fig. 2. The spectra consist of relatively well resolved groups of bands in the visible and infrared spectral range which are associated with transitions from the $^3H_4$, $^4I_{9/2}$, and $^4I_{15/2}$ ground state of Pr^{3+}, Nd^{3+} and Er^{3+}, respectively, to the excited states marked on the picture. Apart of absorption bands characteristic of the optically active rare earth ions, an additional band peaking at about 260 nm is observed for all crystals (including the 'undoped' $K_5LaLi_2F_{10}$ crystal; see the dashed line on Fig. 2). The origin of this absorption is not clear yet; it could be due to lattice point defects as observed in some crystals [15] or to charge transfer transitions. The presence of this band and probably others

Table 1
Energies of crystal field levels and overall splitting of selected multiplets of Pr^{3+}, Nd^{3+} and Er^{3+} in $K_5LaLi_2F_{10}$ crystal

Multiplet	Energy (cm^{-1})	ΔE (cm^{-1})	Component number (theor./exp.)
Pr^{3+} ion in $K_5PrLi_2F_{10}$ crystal			
$^3H_4$	0, 72, 123, 149, 297, 410, 535, 683	683	9/8
$^3H_5$	2192, 2250, 2265, 2298, 2464, 2579, 2610	418	11/7
$^3H_6$	4316, 4377, 4391, 4414, 4446, 4528, 4615, 4855	539	13/8
$^3F_2$	5096, 5165, 5176, 5249, 5410	314	5/5
$^3F_3$, $^3F_4$	6470, 6536, 6565, 6579, 6905, 6933, 7138, 7390	920	15/8
$^1G_4$	9718, 9785, 9921, 10110	392	9/4
$^1D_2$	16677, 16955, 17004, 17047, 17091	414	5/5
$^3P_0$	20855		1/1[a]
$^3P_1$ ($^1I_6$)	21354, 21370, 21393, 21427, 21500	146	3 (13)/5[a]
$^3P_2$	22543, 22594, 22619	76	5/3
Nd^{3+} ion in $K_5NdLi_2F_{10}$ crystal			
$^4I_{9/2}$	0, 128, 169, 291, 333	333	5/5
$^4I_{11/2}$	1963, 2004, 2044, 2056, 2169, 2200	237	6/6
$^4F_{3/2}$	11508, 11550	42	2/2
Er^{3+} ion in $K_5La_{0.95}Er_{0.05}Li_2F_{10}$ crystal			
$^4I_{15/2}$	0, 28, 63, 94, 135, 224, 281, 494	494	8/8
$^4I_{13/2}$	6536, 6566, 6605, 6647, 6698, 6733, 6765	229	7/7
$^4I_{11/2}$	10235, 10267, 10320, 10345, 10395, 10405	170	6/6
$^4I_{9/2}$	12385, 12517, 12559, 12636, 12667	282	5/5
$^4F_{9/2}$	15272, 15322, 15386, 15449, 15521	250	5/5
$^4S_{3/2}$	18416, 18481	65	2/2

[a] Some satellite lines of a low intensity are present in this spectral range.

located at higher energies makes the estimation of matrix absorption edge difficult, however, in any case it is situated below 200 nm.

The emission properties of $K_5PrLi_2F_{10}$ and of $K_5La_{0.98}Pr_{0.02}Li_2F_{10}$ single crystals investigated by us are in general similar to those described in Ref. [13] for polycrystalline samples. From absorption and emission measurements carried out at 5 K we have determined the positions of Pr^{3+} energy levels more accurately, although still not all of the expected Stark components were intense or resolved well enough to determine their exact position. The positions of energy levels are gathered in Table 1. The 'fully concentrated' $K_5PrLi_2F_{10}$ crystal shows the emission from the $^3P_0$ and from thermally populated $^3P_1$ levels only. The emission from the $^1D_2$ level is quenched at any temperature independent on the excitation (either to the $^3P_0$ or resonant to the $^1D_2$ level). The quenching takes place probably via cross relaxation processes $(^1D_2 \rightarrow {}^1G_4) + (^3H_4 \rightarrow {}^3F_{3,4})$ or $(^1D_2 \rightarrow {}^3F_{3,4}) + (^3H_4 \rightarrow {}^1G_4)$ in which the assistance of phonons is not required due to the energy levels scheme. We did not observe the emission from the resonant excited $^1G_4$ level, either at $\approx$1 μm ($^1G_4 \rightarrow {}^3H_4$) or at $\approx$1.3 μm ($^1G_4 \rightarrow {}^3H_5$). In Fig. 3, the emission spectrum from the $^3P_0$ level recorded at 5 K is presented. The lifetime of the $^3P_0$ level is about 33 μs at 5 K and strongly decreases with temperature to $\approx$700 ns at RT. For the 'diluted' $K_5La_{0.98}Pr_{0.02}Li_2F_{10}$ crystal, the emission from $^3P_0$, $^3P_1$ as well as from $^1D_2$ levels were observed. Also a very weak emission due to the $^1G_4 \rightarrow {}^3H_4$ transition was observed after resonant excitation. The emission lifetimes of both the $^3P_0$ and $^1D_2$ levels decrease about 20% with the temperature increase from 5 K to RT (see Table 2).

Our results suggest the presence of both temperature-dependent and -independent cross-relaxation processes in this type of crystal for a wide concentration range. Similar situation was observed for ultraphosphates ($La_{1-x}Pr_xP_5O_{14}$) containing Pr^{3+} ions [16], where the Pr–Pr interactions are still active for Pr^{3+} concentrations as low as 1% ($x = 0.01$). Another effect common to these materials is the presence of a satellite structure observed in the low temperature absorption spectrum, mainly within the $^3H_4 \rightarrow {}^3P_0$ line. Further investigations of the concentration and temperature emission quenching are needed to explain the mechanisms of the interaction mechanisms and of possible collective excitation phenomena in these systems.

The luminescence of $K_5NdLi_2F_{10}$ and Er^{3+} doped

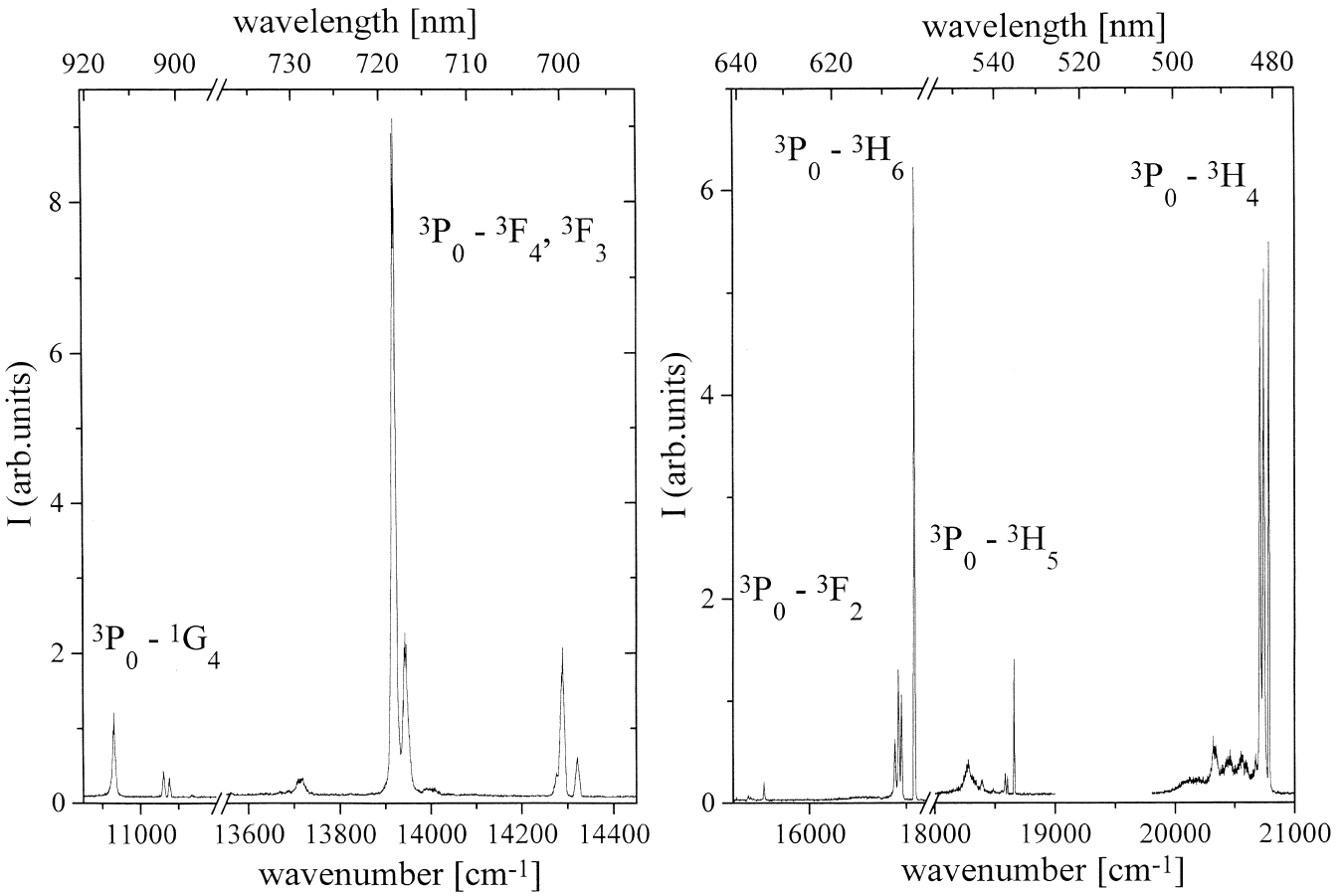

Fig. 3. Luminescence spectrum of $K_5PrLi_2F_{10}$ crystal associated with transitions from the $^3P_0$ level of Pr^{3+} ($\lambda_{exc} = 436$ nm OPO, $T = 5$ K).

Table 2
Emission lifetimes of some excited states of Pr^{3+}, Nd^{3+} and Er^{3+} in $K_5LaLi_2F_{10}$ crystals

Multiplet	Emission lifetime	
	5 K	300 K
Pr^{3+} ion in $K_5La_{0.98}Pr_{0.02}Li_2F_{10}$ crystal		
$^3P_0$	52 μs	33 μs
$^1D_2$	305 μs	250 μs
Pr^{3+} ion in $K_5PrLi_2F_{10}$ crystal		
$^3P_0$	33 μs	0.7 μs
Nd^{3+} ion in $K_5NdLi_2F_{10}$ crystal		
$^4F_{3/2}$	69.9 μs	59.9 μs
Er^{3+} ion in $K_5La_{0.95}Er_{0.05}Li_2F_{10}$ crystal		
$^4S_{3/2}$	0.459 ms	0.442 ms
$^4I_{11/2}$	3.75 ms	2.70 ms
$^4I_{9/2}$	0.450 ms	0.450 ms

$K_5LaLi_2F_{10}$ was studied on single crystals at 300 and 5 K. Low temperature emission of $K_5NdLi_2F_{10}$ is presented in Fig. 4. Two emission bands are associated with transitions from the lowest Stark component of the $^4F_{3/2}$ level to the $^4I_{9/2}$ ground state and the $^4I_{11/2}$ excited state. Luminescence spectra give insight into the Stark level structure of the terminal states. For the $^4F_{3/2} \rightarrow {}^4I_{11/2}$ transition we observe six, sharp and well-resolved lines located at 9542, 9501, 9461, 9449, 9335 and 9306 cm^{-1}. Notable is the dominance of the line at 9542 cm^{-1} (1048 nm). The $^4F_{3/2} \rightarrow {}^4I_{9/2}$ transition consists of four lines giving information about crystal field components position of the $^4I_{9/2}$ ground state. The comparison of the emission spectrum with the absorption one at 300 K allowed us to assign the very weak line at 11 502 cm^{-1} as the missing component due to $^4F_{3/2}(1) \rightarrow {}^4I_{9/2}(1)$ transition. High Nd concentration (3.6×10^{21} ions cm^{-3}) activates a strong self-absorption process thus the intensity of the $^4F_{3/2}(1) \rightarrow {}^4I_{9/2}(1)$ transition is very low. The measured lifetime of the $^4F_{3/2}$ emitting level is 70 μs at 5 K and 60 μs at room temperature. These values are much lower than reported in Ref. [11] (300 μs at 300 K) suggesting the presence of OH^- groups in our crystals, which significantly contribute to the quenching processes.

Low temperature emission of Er^{3+} in $K_5LaLi_2F_{10}$ is presented in Fig. 5. The upper layer shows emission from

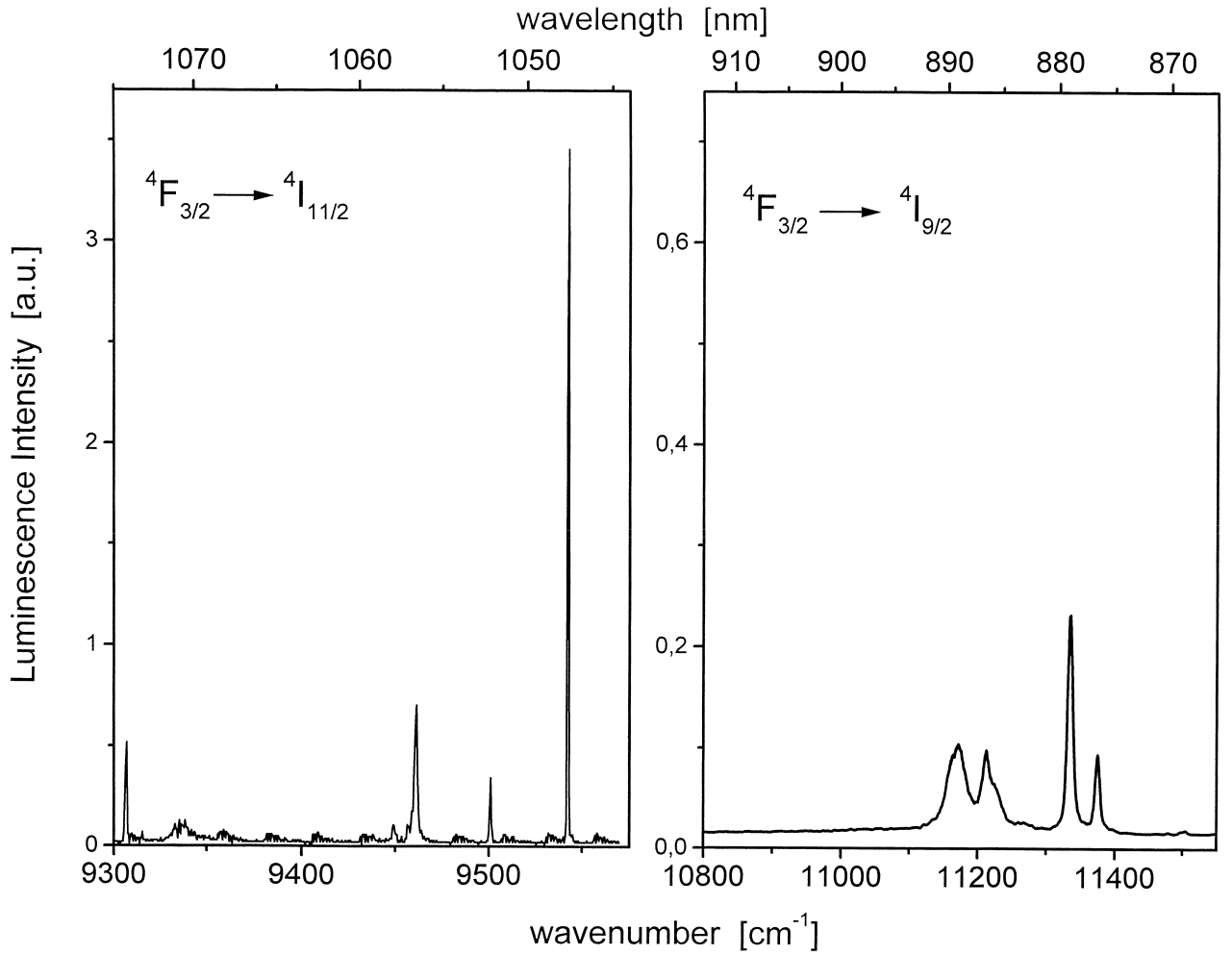

Fig. 4. Luminescence spectra of $K_5NdLi_2F_{10}$ crystal associated with the $^4F_{3/2} \rightarrow {}^4I_{15/2}$ and the $^4F_{3/2} \rightarrow {}^4I_{11/2}$ transitions (λ_{exc}=513 nm OPO, T=5 K).

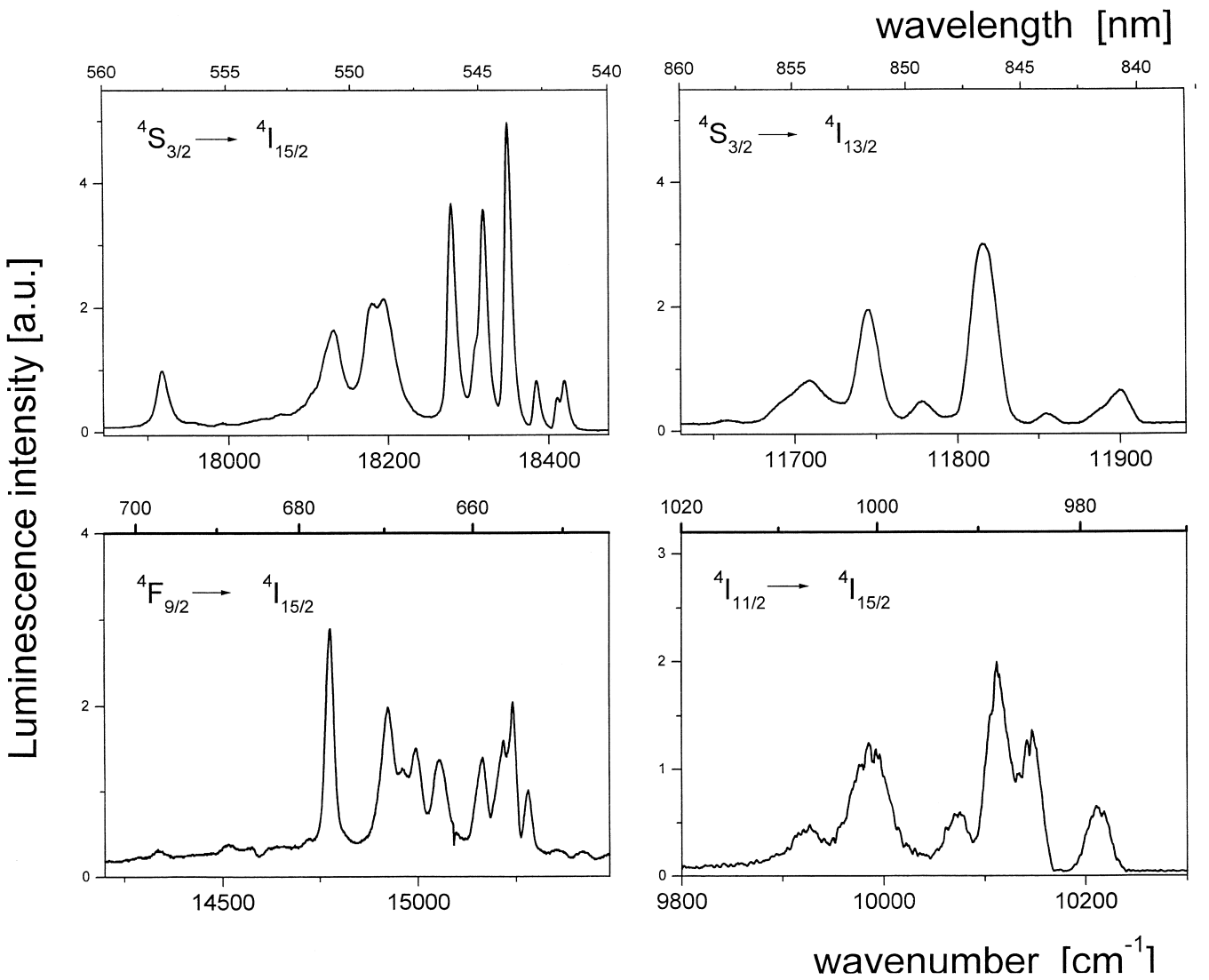

Fig. 5. Luminescence spectra of Er^{3+} in $K_5LaLi_2F_{10}$ crystal recorded at 5 K (λ_{exc}=514 nm Ar line).

the $^4S_{3/2}$ excited state to the $^4I_{15/2}$ ground state and to the $^4I_{13/2}$ excited multiplet. Emission lines observed at about 15 000 cm^{-1} are assigned to the $^4F_{9/2}\rightarrow{}^4I_{15/2}$ transition and luminescence spectrum associated with the $^4I_{11/2}\rightarrow{}^4I_{15/2}$ one appears near 1 μm. We were not able to measure emission from the $^4I_{13/2}$ state that occurs at about 1.6 μm because of experimental limitations. This limitation did not allow us to verify the presence of the interstate fluorescence $^4I_{11/2}\rightarrow{}^4I_{13/2}$ expected in the 2.7–2.9 μm spectral range.

The lifetime measurements of the emitting levels of Er^{3+} ions have been made at 5 and 300 K. Results are gathered in Table 2. The $^4I_{9/2}$ lifetime is temperature independent. It can be seen that unlike the $^4S_{3/2}$ lifetime the temperature influences the lifetime of the $^4I_{11/2}$ level. Taking into account the highest phonon energy (ω_{ph}=685 cm^{-1}) and the energy gap between the $^4I_{11/2}$ level and the lower lying $^4I_{13/2}$ state of 3700 cm^{-1}, we suppose that the multiphonon processes are active. Contribution of ion–phonon and ion–ion interaction to the relaxation of excited states of Er^{3+} in $K_5LaLi_2F_{10}$ is to be determined. For further research, crystals containing lower Er^{3+} concentrations are being prepared.

4. Conclusions

We have grown $K_5LaLi_2F_{10}$ single crystals, both undoped as well as doped, with trivalent praseodymium, neodymium and erbium ions substituting La^{3+} ions in the host. The crystal structure was confirmed and vibrational analysis made. The highest energetic vibrations are of the order of 685 cm^{-1} and are associated with the Li–F stretching vibrations.

The presented optical properties of rare earth dopants are only preliminary results; growth and investigations of the crystals with other dopant concentrations are being carried out. However, in spite of expected weak ion–ion

interactions in this type of crystals with large RE ion separation distance, our results confirm previous predictions about the crucial role of other conditions governing the self-quenching processes.

References

[1] H.G. Danielmeyer, Stoichiometric laser materials, in: Festkörperprobleme, Advances in Solid State Physics, Vol. 15, Pergamon Nieweg, Braunschweig, 1975, p. 253.
[2] H.Y.-P. Hong, Acta Crystallogr., Sect. B 30 (1974) 486.
[3] H.P. Weber, T.C. Damen, H.G. Danielmeyer, Appl. Phys. Lett. 22 (1973) 534.
[4] A.A. Kaminskii, S.E. Sarkisov, J. Bohm, P. Reiche, D. Schultze, R. Uecker, Phys. Status Solidi (a) 43 (1977) 71.
[5] F. Auzel, J. Dexpert-Ghys, C. Gautier, J. Lumin. 27 (1982) 1.
[6] F. Auzel, Mater. Res. Bull 14 (1979) 223.
[7] A.A. Kaminski, Laser Crystals Their Physics and Properties, 2nd Edition, Springer, Berlin, 1990.
[8] R.T. Wegh, H. Donker, A. Meijerink, R.J. Lamminmäki, J. Hölsä, Phys. Rev. B 56 (1997) 13841.
[9] X. Zhang, J.-P. Jouart, G. Mary, J. Phys. Condens. Matter 10 (1998) 493.
[10] J. Becker, J.Y. Gesland, N.Yu. Kirikova, J.C. Krupa, V.N. Makhov, M. Runne, M. Queffelec, T.V. Uvarova, G. Zimmerer, J. Lumin. 78 (1998) 92.
[11] B.C. McCollum, A. Lempicki, Mater. Res. Bull. 13 (1978) 883.
[12] H.Y.-P. Hong, B.C. McCollum, Mater. Res. Bull. 14 (1979) 137.
[13] A. Lempicki, B.C. McCollum, J. Lumin. 20 (1979) 291.
[14] G. Dominiak-Dzik, S. Gołąb, M. Bałuka, A. Pietraszko, K. Hermanowicz, J. Phys. Condens. Matter 11 (1999) 5245.
[15] N.S. Kovalyova, A.O. Ivanov, E.P. Dubrovina, Kvant. Elektr. 8 (1981) 2433.
[16] H. Dornauf, J. Heber, J. Lumin. 20 (1979) 271.